Imaging Diagnostics of Debris from Laser-Produced Tin Plasma with Droplet Target for EUV Light Source

Daisuke Nakamura[*1], Tomoya Akiyama[*1], Akihiko Takahashi[*2], Tatsuo Okada[*1]

*[*1] Graduate School of Information Science and Electrical Engineering, Kyushu University,*
744 Motooka, Nishi-ku, Fukuoka 819-0395, Japan
E-mail: dnakamura@ees.kyushu-u.ac.jp
*[*2] Graduate School of Medical Sciences, Kyushu University,*
3-1-1 Maidashi, Higashi-ku, Fukuoka 812-8582, Japan

The dynamics of debris from laser-produced tin (Sn) plasma was investigated for a practical extreme ultraviolet (EUV) lithography source. The kinetic behaviors of the Sn atoms and of the dense particles from Sn droplet target irradiated by double pulses from the Nd:YAG laser and the CO_2 laser were also investigated by the laser-induced fluorescence imaging method and a high-speed imaging, respectively. After the pre-pulse irradiation of the Nd:YAG laser, the Sn atoms were ejected in all direction from the target with a speed of as fast as 20 km/s and the dense particle cloud expanded by a reaction force due to the plasma expansion with a speed of approximately 500 m/s. The expanding target was subsequently irradiated by the main-pulse of CO_2 laser and the dense cloud was almost disappeared by main-pulse irradiation.

Keywords: EUV, Laser-produced plasma, Debris, LIF imaging, Shadowgraph

1. Introduction

As the next generation optical lithography for advanced LSI fabrication, an extreme ultraviolet (EUV) light source at 13.5 nm has been developed. In a practical EUV lithography system, it is said that an average EUV power of 180 W in 2 %-bandwidth around 13.5 nm at the intermediate focus is required [1]. EUV light sources have been under development based on the laser-produced plasma (LPP) or the discharge-produced plasma [2]. In the case of LPP, the tin (Sn) plasmas produced by CO_2 lasers at a wavelength of 10.6 μm have been considered to be the most promising EUV light source [3,4]. For Sn target, a conversion efficiency of about 4 % [5,6], which is higher than any other material, such as xenon (Xe) or lithium (Li), has been obtained. However, the generation of debris that damages collector optics and limits the lifetime of the optical system is more critical problem in the case of Sn. Therefore, a mitigation of the debris is of importance for the development of a practical EUV lithography system. Although several methods have been developed for the debris mitigation, including a magnetic field trap of ions [7], foil trap [8], and so on [9], it is difficult to mitigate the neutral particle debris because they can not be controlled by electromagnetic field. In the previous study, it was found that the neutral atoms are originated from the low-intensity part of the laser spot and the deep layer from the target surface [10] and large size debris must be also generated from the same parts. So, the fundamental and general approach for debris mitigation is the use of a minimum amount of Sn that can provide a sufficient EUV power. This type of the Sn target is called as a mass-limited or a minimum-mass target [6,11-13].

One of the most practical structures for a minimum-mass target considering the target supply at a high repetition rate of 10-100 kHz is Sn droplets with a size of several tens of micrometers in diameter. In the use of the droplet target and CO_2 laser, however, it is required that Sn micro-droplets have to be expanded by 10-20 times before CO_2 laser irradiation, in order to improve the coupling efficiency between long-wavelength CO_2 laser and micro-droplets. For the purpose, the pre-irradiation of a Q-switched Nd:YAG laser at a wavelength of 1064 nm prior to the main CO_2 laser irradiation is one of the promising schemes. This scheme is called the double pulse irradiation (DPI) technique [14]. In the DPI scheme, the ablation dynamics of laser-irradiated Sn droplet are very important for attempting to optimize DPI operation and mitigate the debris.

In this report, we describe the ablation dynamics of a Sn droplet irradiated by double laser pulses from a Nd:YAG laser and a CO_2 laser. The spatial distribution of the Sn atoms from the Sn plasma was visualized by the laser-induced fluorescence (LIF) imaging method. While, the temporal behavior of dense particles from the droplet were visualized in synchronized with LIF imaging using a high-speed framing camera in single ablation event.

2. Experiment

2.1 Experimental Setup

The experimental setup for investigation of the debris is shown in Fig. 1. It consists of a Q-switched Nd:YAG laser (Continuum Powerlite8000) as a driver laser, a vacuum chamber with a target holder, and time-resolved two-dimensional LIF imaging and shadowgraph imaging systems. An output energy of the Nd:YAG laser was 1 J with a Q-switched pulse of 8 ns in FWHM at a wavelength of 1.06 μm. The laser intensity was estimated to be 5×10^{11} W/cm^2. The Sn droplets were made with a help of a pulsed-laser irradiation and the droplet was attached to a
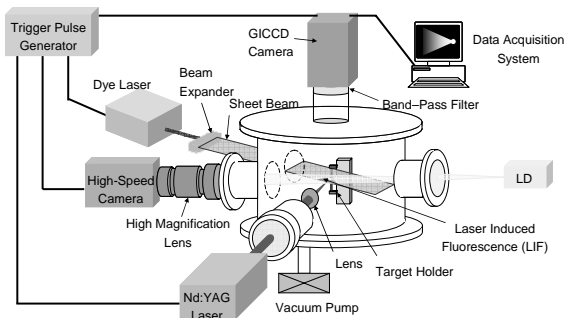
Fig. 1 Experimental setup for debris imaging.

polyamide fiber of 10 μm diameter as the target for laser irradiation. The Nd:YAG laser beam was aligned at a normal incidence on the target surface. The chamber was evacuated at a pressure of 10^{-3} Pa by a vacuum pump. In the LIF imaging for Sn atoms, a planar sheet laser beam from a tunable dye laser (Spectra-Physics Sirah) pumped by the third harmonics of a Q-switched Nd:YAG laser (Spectra-Physics LAB-150) was passed in the plane of the target. More detailed information about LIF imaging has been described in the previous report [10].The shadowgraph images were captured by a high-speed framing camera (Hadland Photonics Ltd. Imacon468) with a back-light from a cw laser diode (Sacher Lasertechnik littrow TEC-120) at a wavelength of 848 nm. The camera was triggered by the pulse generator in synchronizing with the LIF system and the gate width was set to 100ns.

2.2 Kinetic behavior of neutral atom debris

Fig. 2 shows the temporal changes in the spatial distribution of Sn atoms at different delay times after laser irradiation from the droplet target by LIF imaging, where the droplet size was 30 μm in a diameter and the target was located at the center of the image before the irradiation. The fluorescence at 317.50 nm was observed by a gated ICCD camera (Roper Scientific PIMAX) through a band-pass filter. In this experiment, since the beam spot size of the Nd: YAG laser was approximately 100 μm in a diameter, which was larger than the droplet target, a part of the beam passed outside of the target. It was observed that the Sn atoms were emitted in all direction from the target. The kinetic speed of the Sn atoms at the expanding front was estimated to be approximately 20 km/s from the image of 400 ns delay. The directional distributions of the ejected species are generally governed by the curvature of the target surface. In the case of the flat plate target, Sn atoms are ejected along the target surface normal due to steep pressure gradient, and results in the forward-peaked distribution. In the case of the micro-droplet target, on the other hand, it is considered that since the size of the laser-produced plasma was larger than the curvature of the target surface, the Sn atoms were ejected to the opposite side of the target due to the collision during plasma expansion.
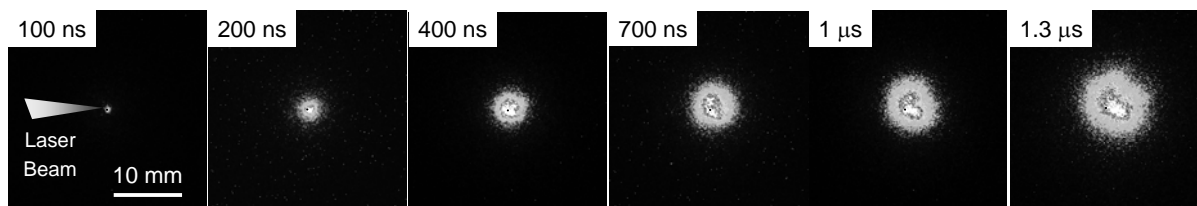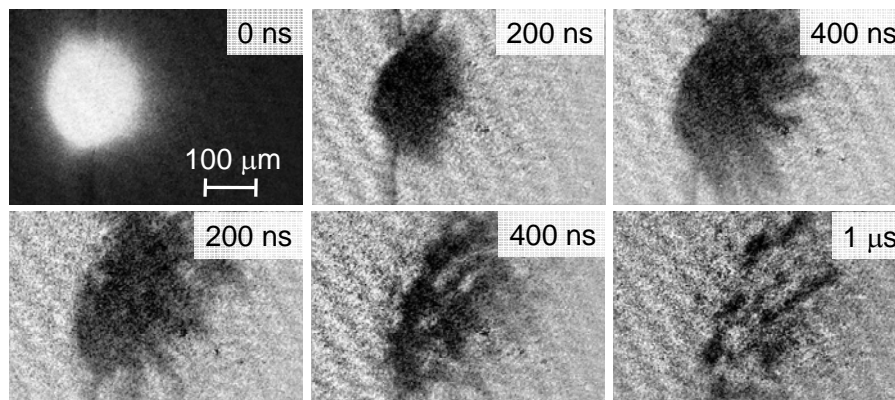
2.3 Shadowgraph of dense particles irradiated by pre-pulse

Fig. 3 shows the shadowgraph images at different delay times after pre-pulse irradiation. The Nd:YAG laser beam was irradiated onto the droplet from the left hand side of the image. The images were captured by the high-speed framing camera with the gate width of 100 ns at a normal angle from the laser incidence, simultaneously with the LIF imaging. In the image of 0 ns, only the plasma radiation was observed. The fiber that sustained the droplet was cut instantaneously by the laser-produced plasma. After 100 ns, the dense particle cloud, that may consisted of small molten Sn particles or clusters, moved to the right hand side of the image by a reaction force from due to the plasma expansion and the drift velocity was estimated to be approximately

Fig. 2 The temporal changes in the spatial distribution of Sn atoms from the droplet target with a diameter of 30 μm at different delay times after laser irradiation.

Fig. 3 The shadowgraphs of the irradiated target debris at different delay times after pre-pulse irradiation.
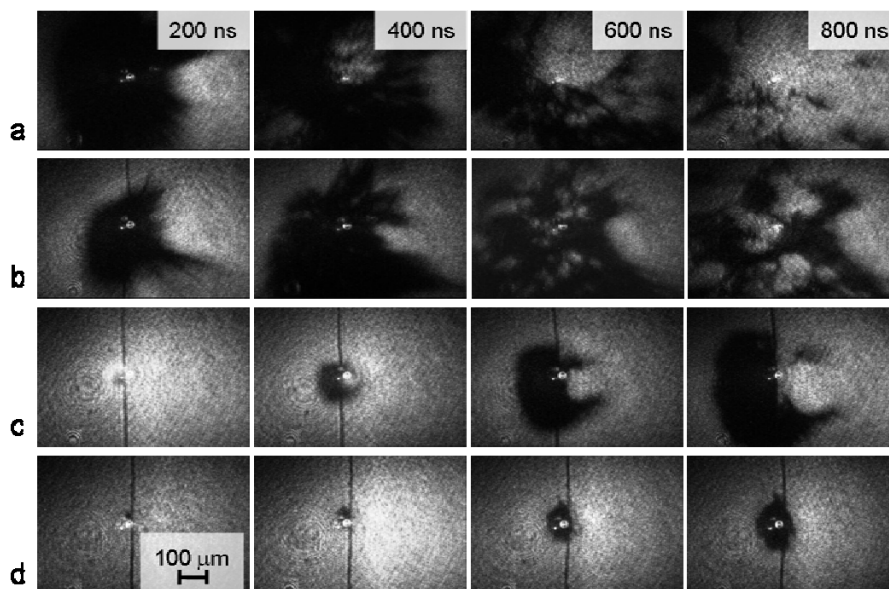
Fig. 4 The shadowgraphs of the irradiated target debris at the pre-pulse intensities of (a) 1.1×10^{12}, (b) 4.8×10^{11}, (c) 1.6×10^{11}, and (d) 3.4×10^{9} W/cm^2.

500 m/s. After delay times of 800 ns to 1 µs, the dense cloud at early delay was gradually vanished by expansion and vaporization. We believe that the vaporization of the dense cloud is responsible for the production of Sn atoms observed at larger delays in Fig.2. As the cloud was vanished, the small particulates became visible as small dots in Fig.3. These particulates were collected on a witness plate mounted 15 mm behind the target. Several dozen particulates were collected on the surface of the witness plate. The volume of the particulates was measured using an atomic force microscope and converted to the diameter of the sphere that has the same volume of particulates. In result, the estimated diameter was in the range of about 1-6 µm. Thus, it was confirmed that neutral atoms and small liquid debris were generated from the droplet target irradiated by single pulse of Nd:YAG laser. It was also checked that the dense cloud and the particulates in Fig. 3 were not from the fiber, but from the Sn droplet, by comparing the images with and without the Sn droplet on the fiber.

Next, an influence of the pre-pulse intensity on the ablation dynamics was investigated. Fig.4 shows the shadowgraphs of the irradiated target at different intensities of pre-pulse, where an injection seeded Nd:YAG laser (Spectra Physics, Quanta-Ray Pro), which has a spot size of approximately 40 µm, was used. And the observation direction was 135 degrees from the laser beam incidence as shown in Fig.5 due to preparing for DPI scheme. The expanding speed of the dense cloud increases with increasing the intensity of the pre-pulse. At the intensity of 1.1×10^{12} W/cm^2, the dense cloud was expanded more than the observation area at 200 ns after laser irradiation. And the cloud seems to disappear from its central part because of the plasma expansion. In Fig4 (d), on the other hand, the cloud was expanded to about 100 µm after 800 ns delay. The target was hardly expanded at lower intensity than that of Fig.4 (d).

2.4 Shadowgraph of dense particles irradiated by double pulses
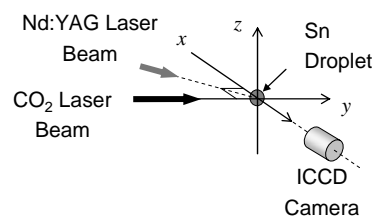
Fig. 5 Spatial configuration for double pulse irradiation.

The ablation dynamics of the target by double pulses of Nd:YAG and CO$_2$ laser was subsequently investigated. The pre-pulse of Nd:YAG laser irradiated the droplet target with a fluence of 2.0×10^{11} W/cm^2, which was derived from the results of Fig.4 to expand the target within 1 µs sufficiently. CO$_2$ laser (Lambda Physik EMG201MSC) beam with a gain switched pulse of 50 ns in FWHM followed by a low-intensity tail lasting for about 1 µs was used as the main-pulse. Fig.5 shows the spatial configuration of double pulse irradiation. The both beams were in the x-y plane and the angle between the two beams was 45 degrees. The main-pulse of CO$_2$ laser irradiated the dense cloud after pre-pulse irradiation with a fluence of 1.6×10^{9} W/cm^2. A delay time of the main-pulse was proposed to be 800 ns, that the dense cloud expanded by the pre-pulse had almost the same size as that of the CO$_2$ laser beam. Fig.6 shows the Sn droplet target irradiated by the double pulses at different delay times after pre-pulse irradiation. At a delay of 800 ns, the plasma radiation produced by CO$_2$ laser irradiation was observed. At 600 ns, the dense cloud was observed as in Fig.4(c), but after CO$_2$ laser irradiation the dense cloud disappeared. Thus it was found that the DPI scheme was also useful the mitigation of the particulates. Regarding the mitigation of Sn atoms, on the other hand, it should be noticed that the fast Sn atoms were already expanded around about 8 mm in diameter even at the delay of 400 ns, as shown in Fig.2. Therefore, Sn atoms are inevitably generated, as long as the Q-switched Nd:YAG laser is used as the pre-pulse laser in order to expand the target within 1 µs in the DPI scheme. In addition, the expansion speed limits the
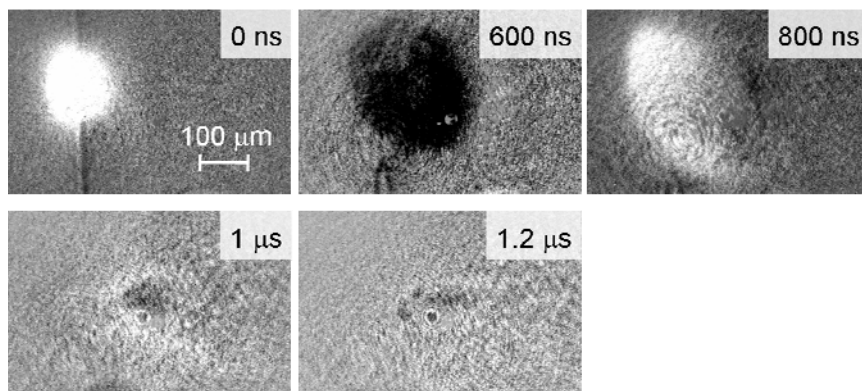
Fig. 6 The shadowgraphs of the target irradiated by the double pulses of Nd:YAG laser and CO_2 laser at different delay times.

repetition rate in DPI scheme. The expansion condition of the dense cloud strongly depends on the pre-pulse energy that hit the target, as shown in Fig.4. At low intensity, more time is required before the dense cloud expands up to the size of the CO_2 laser beam.

2.5 Beam position dependence of the target expansion direction

Finally, the beam position dependence of the target expansion direction was investigated. It is desirable that the spot size of the pre-pulse laser is almost the same as the target size for high coupling efficiency between the laser and the target. However, the distribution of the dense cloud generated by pre-pulse strongly depends on the irradiation position of the beam with smaller spot size. Fig.7 shows the shadowgraph of the dense cloud at the 300 ns delay from the pre-pulse irradiation when the target position was changed, where the target position before irradiation was (a) -15 μm, (b) 0 μm, (c) 15 μm, (d) 30 μm and (e) 60 μm. In Fig.7(a), (c), (d), the dense cloud was shifted to downward or upward in the image. In Fig.7(e), on the other hand,
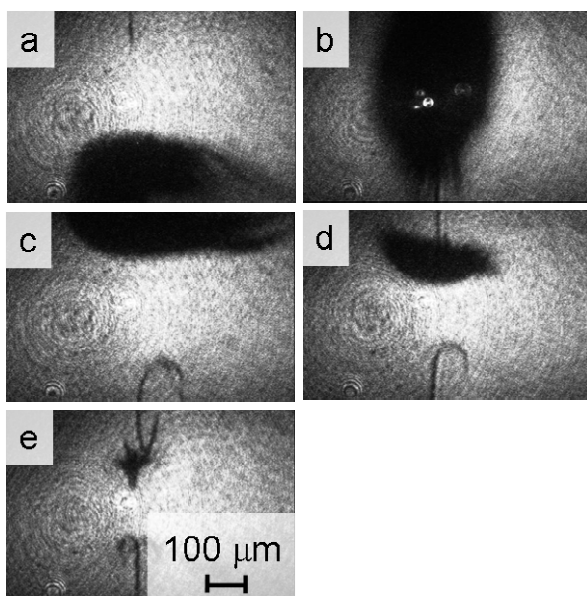
the laser beam not irradiated any longer, the target was hardly expanded. This result indicates that the irradiation position is important for the distribution of the dense cloud in DPI scheme and an alignment of the beam and the target becomes a problem at high-repetition rate operation.

3. Conclusions

The ablation dynamics of the Sn micro-droplet in the DPI scheme for EUV lithography source was investigated by the LIF imaging system and the shadowgraph framing system. In the present DPI, a Q-switched Nd:YAG laser and a CO_2 laser are used as a pre-pulse for the target expansion and a main-pulse for the plasma production, respectively. It was found that the fast Sn atoms are ejected in all directions with a speed of as fast as 20 km/s by pre-pulse irradiation and the dense Sn cloud expands with a speed of about 500 m/s. The expanding speed of the dense cloud increases with increasing the intensity of the pre-pulse. It takes about 800 ns for the micro Sn droplet to expand to the size of around 500 μm in diameter with a fluence of 2.0×10^{11} W/cm² before the main-pulse irradiation. After CO_2 laser irradiation the dense cloud disappeared. On the other hand, however, Sn atoms are inevitably generated, as long as the Q-switched Nd:YAG laser is used as the pre-pulse laser in the DPI scheme, in order to expand the target to a comparable size as the main CO_2 laser beam within 1 μs. Furthermore, the alignment of the pre-pulse beam and the target is important for the distribution of the dense cloud in DPI scheme.

References
[1] U. Stamm: J. Phys. D 37, (2004) 3244.
[2] V. M. Borisov, A. V. Eltsov, A. S. Ivanov, Y. B. Kiryukhin, O. B. Khristoforov, V. A. Mishchenko, A. V. Prokofiev, A. Y. Vinokhodov, V. A. Vodchits: J. Phys. D 37, (2004) 3254.

Fig. 7 The shadowgraphs of the dense cloud at the 300 ns delay from the pre-pulse irradiation when the target position was changed. The target position before irradiation was (a) -15 μm, (b) 0 μm, (c) 15 μm, (d) 30 μm and (e) 60 μm.

[3] H. Tanaka, K. Akinaga, A. Takahashi, T. Okada: Jpn. J. Appl. Phys. 43, (2004) L585.

[4] H. Tanaka, A. Matsumoto, K. Akinaga, A. Takahashi, T. Okada: Appl. Phys. Lett. 87, (2005) 041503.

[5] S. Fujioka, M. Shimomura, Y. Shimada, S. Maeda, H. Sakaguchi, Y. Nakai, T. Aota, H. Nishimura, N. Ozaki, A. Sunahara, K. Nishihara, N. Miyanaga, Y. Izawa and K. Mima: Appl. Phys. Lett. 92, (2008) 241502.

[6] Y. Ueno, G. Soumagne, A. Sumitani, A. Endo and T. Higashiguchi: Appl. Phys. Lett. 91, (2007) 231501.

[7] H. Komori, Y. Imai, G. Soumagne, T. Abe, T. Suganuma, Akira Endo: Proc. SPIE 5751, (2005) 859.

[8] L. A. Shmaenok, C. C. de Bruijn, H. F. Fledderus, R. Stuik, A. A. Schmidt, D. M. Simanovski, A. V. Sorokin, T. A. Andreeva, F. Bijkerk, Proc. SPIE 3331, (1998) 90.

[9] D. Nakamura, H. Tanaka, K. Tamaru, Y. Hashimoto, A. Takahashi, T. Okada: J. Appl. Phys. 102, (2007) 123310.

[10] H. Tanaka, Y. Hashimoto, K. Tamaru, A. Takahashi, T. Okada: Appl. Phys. Lett. 89, (2006) 181109.

[11] S. Namba, S. Fujioka, H. Nishimura, Y. Yasuda, K. Nagai, N. Miyanaga, Y. Izawa, K. Mima, K. Takiyama: Appl. Phys. Lett. 88, (2006) 171503.

[12] M. Richardson, C. S. Koay, K. Takenoshita, C. Keyser: J. Vac. Sci.Technol. B 22, (2004) 785.

[13] M. Shimomura, S. Fujioka, T. Ando, H. Sakaguchi, Y. Nakai, Y. Yasuda, H. Nishimura, K. Nagai, T. Norimatsu, K. Nishihara, N. Miyanaga, Y. Izawa, K. Mima: Appl. Phys. Exp. 1, (2008) 056001

[14] T.Higashiguchi, N. Dojyo, M. Hamada, K. Kawasaki, W. Sasaki, S. Kubodera: Proc. SPIE 6151, (2006) 615145.